

Transient x-ray absorption spectroscopy of hydrated halogen atom

Christopher G. Elles,^{a)} Ilya A. Shkrob,^{b)} and Robert A. Crowell^{c)}
Chemistry Division, Argonne National Laboratory, Argonne, Illinois 60439, USA

Dohn A. Arms and Eric C. Landahl
Advanced Photon Source, Argonne National Laboratory, Argonne, Illinois 60439, USA

(Received 20 September 2007; accepted 30 November 2007; published online 11 February 2008)

Time-resolved x-ray absorption spectroscopy has been used to observe the transient species generated by one-photon detachment of an electron from aqueous bromide. The *K*-edge spectrum of the short-lived Br^0 atom exhibits a resonant $1s-4p$ transition that is absent for the Br^- precursor. The strong $1s-4p$ resonance suggests that there is very little charge transfer from the solvent to the open-shell atom, whereas weak oscillations above the absorption edge indicate that the solvent shell around a neutral Br^0 atom is defined primarily by hydrophobic interactions. These conclusions are in agreement with Monte Carlo and quantum chemical simulations of the solvent structure. © 2008 American Institute of Physics. [DOI: [10.1063/1.2827456](https://doi.org/10.1063/1.2827456)]

Reactions of small inorganic radicals in aqueous solution are important for aerosol, marine, photo- and radiation chemistry. The reactivity of such radicals depends on their interaction with polar water molecules. As there are a limited number of experimental methods for studying the hydration of short-lived radicals lacking a strong chromophore, new techniques capable of yielding direct structural information with atomic resolution are required. Time-resolved x-ray scattering¹ and x-ray absorption spectroscopy²⁻⁷ (XAS) are such techniques. In this Communication, we report the study of the hydration of a simple open-shell system, the Br^0 atom, using transient XAS.

Details about the hydration of halogen atoms are not well known.^{2,3} The hydration of halogen atoms (X^0) is very different from the hydration of negatively charged halide anions (X^-). Whereas the anion forms strong hydrogen bonds with several water molecules in the first solvent shell [Fig. 1(a)], hydrophobic effects dominate the solvation of neutral halogen atoms [Fig. 1(b)]. The bromine atom resides in a solvent cavity and interacts with the solvent to give a charge transfer (CT) absorption band at 4.6 eV.⁸ The CT absorption promotes an electron from the water molecule(s) onto the halogen atom [Fig. 1(c)]. In the case of Cl^0 , electron spin resonance measurements⁹ suggest that the Cl^0 atom and one of the water molecules form a two center, three electron ($\sigma^2\sigma^*1$) bond in the ground state. Similar bonding may also occur for Br^0 and I^0 in water.¹⁰ The much stronger halogen-halogen bonding between a halogen atom and its anion is also a two center, three electron bond [Fig. 1(d)].

Recently, Pham *et al.*⁷ reported XAS measurements of I^0 atoms following biphotonic electron detachment from aqueous iodide. They observe a prominent change of the spectra at the L_1 and L_3 absorption edges, but their interpretation is

complicated by the reaction of I^0 with excess I^- to form a substantial amount of I_2^- and I_3^- within the ~ 80 ps duration of the x-ray pulse. Rapid formation of molecular anions in their experiment is a consequence of the high concentration of I^- (500 mol/m^3), which is necessary to overcome inefficient two-photon absorption. In contrast, efficient one-photon electron detachment from Br^- at 200 nm (Ref. 11) and strong absorption at the *K* edge of bromine allow us to use dilute aqueous solutions in which the reaction of Br^0 with excess anions is much slower.

The present experiment uses the laser pump-x-ray probe capabilities of beamline 7ID of the Advanced Photon Source at Argonne. Fourth harmonic generation of the output from an amplified Ti:sapphire laser provides $5 \mu\text{J}$ pulses of 200 nm light with a repetition rate of 1 kHz. A MgF_2 lens focuses the ultraviolet light to a diameter of $95 \mu\text{m}$ at the sample, where it crosses the x-ray beam at an angle of 4° . The laser is synchronized with the synchrotron by an active feedback control loop that adjusts the laser oscillator cavity length. The relative delay between laser and x-ray pulses is controlled electronically. The synchrotron provides tunable x-ray pulses with a duration of ~ 80 ps and a repetition rate of 6.54 MHz (24 bunch mode). X rays from the undulator pass through a tunable diamond monochromator ($\Delta E/E = 5 \times 10^{-5}$) before a Kirkpatrick-Baez mirror pair focuses them to a spot size of about $25 \mu\text{m}$ in the sample. The sample is a $100 \mu\text{m}$ thick liquid jet of $5-10 \text{ mol/m}^3$ NaBr solution with the flat surface of the jet rotated 45° relative to the x-ray beam. Se filters absorb elastically scattered x rays and a gated avalanche photodiode detector on each side of the jet monitors the bromine K_α fluorescence. We record fluorescence count rates for the two x-ray pulses immediately following the laser pulse ($\Delta t, \Delta t + 153 \text{ ns}$) and normalize the signal to account for variations of the x-ray flux. Scanning the incident energy gives the spectra at each delay time.

Figure 2(a) compares the static spectrum of the bromide solution with the transient spectrum at 1 ns delay. The conversion of a fraction of Br^- anions to neutral Br^0 atoms by

^{a)}Present address: Department of Chemistry, University of Southern California, Los Angeles, CA 90089. Electronic mail: elles@usc.edu.

^{b)}Electronic mail: shkrob@anl.gov.

^{c)}Present address: Chemistry Bldg. 555, Brookhaven National Laboratory, Upton, NY 11973-5000. Electronic mail: crowell@bnl.gov.

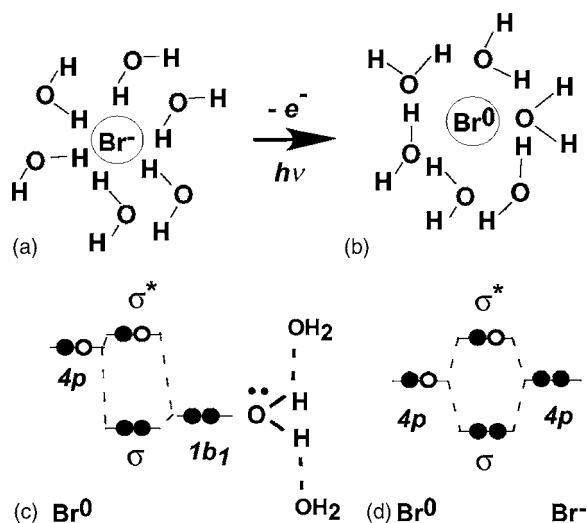


FIG. 1. Sketches of the solvent structure around (a) Br⁻ and (b) Br⁰. Panels (c) and (d) show the schematic orbital diagrams for the Br⁰...OH₂ complex and Br₂⁻, respectively.

the 200 nm laser pulse is evident from the resonant 1s-4p transition below the bromine *K* edge. Subtracting the static spectrum of Br⁻ from the transient spectra at delays of 1 and 154 ns gives the difference spectra $\mu_{\text{on}} - \mu_{\text{off}}$ in Fig. 2(b). The spectra at the two delay times are different because nearly half of the Br⁰ atoms at 1 ns react with excess Br⁻ to form Br₂⁻, while the other Br⁰ atoms recombine with the hydrated electron. Other than Br⁻, the predominant species at 1 and 154 ns are Br⁰ and Br₂⁻, respectively.¹²

The difference spectra in Fig. 2(b) show that the resonant transition in Br₂⁻ is 1.6 eV higher in energy than the

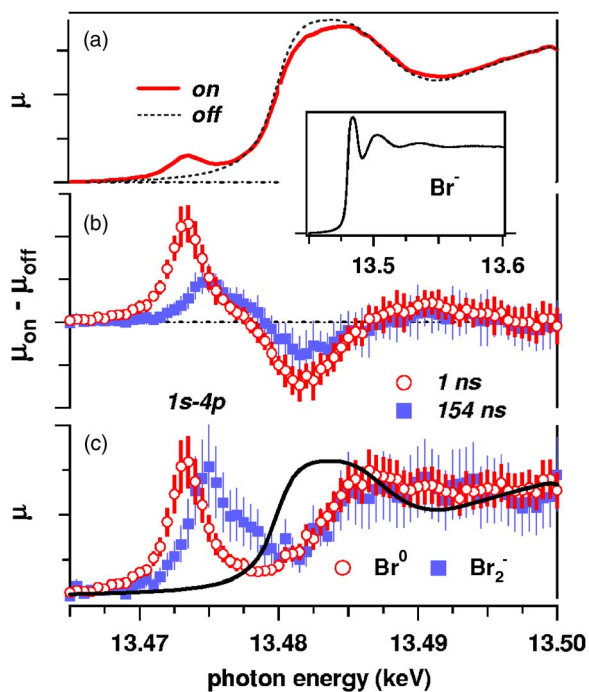


FIG. 2. (Color online) (a) Laser-on and laser-off x-ray absorption spectra of aqueous Br⁻ at $\Delta t = 1$ ns. The inset shows the static (laser-off) spectrum of Br⁻ over a wider energy range. (b) The difference spectra $\mu_{\text{on}} - \mu_{\text{off}}$ at delay times of 1 ns (open circles) and 154 ns (filled squares). (c) Reconstructed spectra of Br⁰ (open circles) and Br₂⁻ (filled squares). The solid line is the absorption spectrum of Br⁻. Vertical bars indicate one standard deviation.

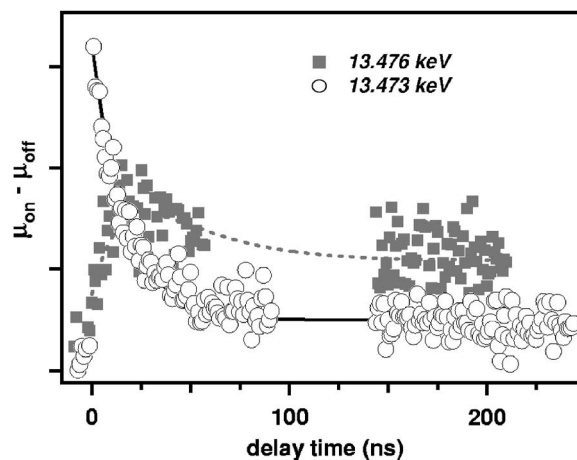


FIG. 3. Transient x-ray absorption difference signals $\mu_{\text{on}} - \mu_{\text{off}}$ for 4.9 mol/m³ solution of NaBr observed at 13.473 keV (open circles) and 13.476 keV (filled squares). The lines are to guide the eye.

transition in Br⁰. Excitation of Br⁰ promotes a 1s electron into the 4p vacancy produced by detaching an electron from Br⁻, whereas the resonant transition for the Br₂⁻ anion excites an electron to a σ^* antibonding orbital [Figs. 1(c) and 1(d)].¹³ The spectral shift of the resonant x-ray absorption energy allows us to observe the reaction kinetics of the transient Br⁰ atom. Figure 3 shows the time-dependent change in absorption at 13.473 and 13.476 keV. Absorption at the lower energy is predominantly due to Br⁰ atoms; therefore, the decay of the x-ray absorbance indicates the loss of Br⁰ atoms as they recombine with hydrated electrons and react with Br⁻. Both Br⁰ and Br₂⁻ contribute to the absorption at 13.476 keV, where the initial increase of the signal is due to production of Br₂⁻ and the slower partial decay is from the Br⁰ contribution. Importantly, these kinetics give an accurate estimate of the product concentrations and thus allow us to reconstruct the spectra of the transient species by subtracting the contribution from Br⁻. Details of the kinetic scheme and calculation of the conversion yields are given as supplemental material.¹² The reconstructed spectra of Br⁰ and Br₂⁻ are shown in Fig. 2(c), along with the static spectrum of Br⁻. The *K*-edge absorption energy is ~ 5 eV higher for the transient species than for bromide. The higher energy for Br⁰ reflects the electrostatic attraction of the outgoing electron to the positively charged core.

Perhaps the most intriguing feature of the recovered x-ray absorption spectrum of Br⁰ is the significantly shallower modulation above the *K* edge relative to the Br⁻ spectrum. A Monte Carlo (MC) simulation of the solvent structure provides helpful insight to understand this difference in the x-ray absorption fine structure (XAFS). The simulation includes 200 simple point charge/flex water molecules¹⁴ and a single Br⁰ or Br⁻ in a supercell, with solute-water interaction potentials from Refs. 15 and 10, respectively. An ensemble of 1500 snapshots at 298 K were taken from 3×10^7 MC steps to give the Br-O radial distribution functions (RDFs), $g_{\text{Br-O}}(r)$, in Fig. 4(a). (The proton contribution to the XAFS spectrum is negligible.) For Br⁻, the narrow peak at 3.2 Å is due to strong hydrogen bonding (Br⁻...H-OH) between the anion and approximately six

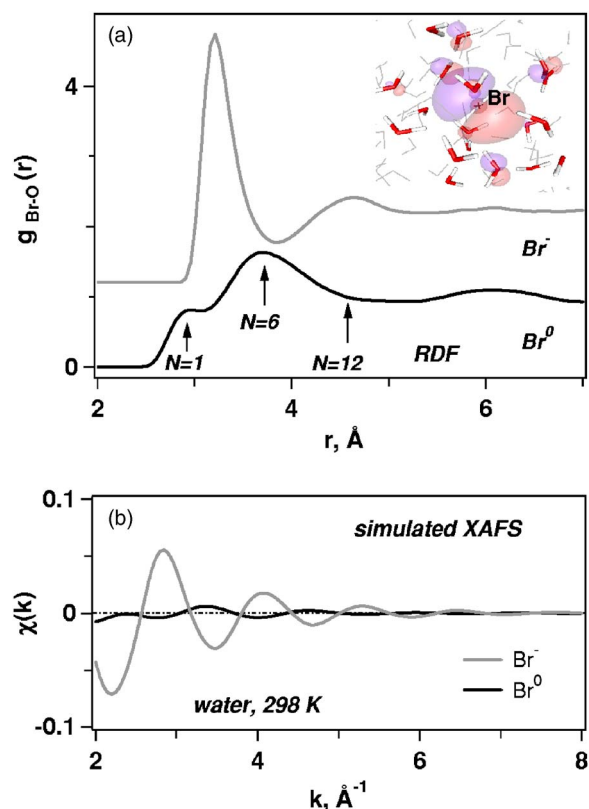


FIG. 4. (Color online) (a) Calculated Br–O RDF for hydrated Br^- and Br^0 . Oxygen coordination numbers N are indicated by arrows. The inset shows the singly occupied orbital of the bromine atom inside the embedded water cluster from our *ab initio* calculations. (b) The simulated XAFS spectra for hydrated Br^- and Br^0 . The first oscillation corresponds to the energy range of Fig. 2(c).

water molecules in the first solvent shell.^{15,16} The RDF for the Br^0 atom lacks this feature because the hydrophobic atom interacts weakly with the solvent. Instead, the atom occupies a nearly spherical cavity formed by 10–12 water molecules that are hydrogen bonded to other water molecules in the first and second solvent shells. The only distinctive feature in this RDF is a shoulder at 3 Å that corresponds to a weak $\text{Br}^0 \cdots \text{OH}_2$ adduct involving a single water molecule. For other water molecules, the Br^0 –O distances are significantly longer, ~ 3.7 Å.

Taking nuclear configurations from the MC ensemble for water molecules with $r(\text{Br}^0\text{--O}) < 8$ Å, we simulate the XAFS spectra of Br^- and Br^0 using the program FEFF8 [Fig. 4(b)].¹⁷ The highly organized hydrogen bonding structure of hydrated Br^- gives deep oscillations in the static spectrum, but the magnitude of the oscillations is approximately ten times smaller for hydrated Br^0 atoms. Although the calculation pertains to higher x-ray energies than the present experiment covers (only the first oscillation is observed experimentally), the modulation is clearly much weaker in the reconstructed spectrum of Br^0 than in the Br^- spectrum [Fig. 2(c)]. The contribution of the $\text{Br}^0 \cdots \text{OH}_2$ adduct to the XAFS spectrum is small compared with the contributions from the other 10–12 oxygen atoms in the first solvent shell.

Pham *et al.*⁷ suggested that significant CT from a water molecule suppresses the $2s$ – $5p$ resonance in the L_1 spectrum of I^0 by as much as 70% relative to the absorption strength

above the edge. No such dramatic suppression of the $1s$ – $4p$ resonance is evident from our K -edge spectrum of Br^0 . Although the relative intensity of the preedge absorption is sensitive to the ratio of Br^0/Br^- that we use to reconstruct the spectrum, the actual Br^0 yield would have to be a factor of 2 higher than we assume in order to give a 20% suppression below the absorption edge. This is unlikely given the close agreement of our calculated photoconversion yield (13%) and the value obtained by fitting the decay of the Br^0 signal in Fig. 3 (12%–15%).

To estimate the degree of CT in the Br^0 -water adduct, water clusters that include all solvent molecules with $r(\text{Br}^0\text{--O}) < 5.5$ Å were extracted from the MC simulation. Water molecules outside of the extracted cluster were replaced by fractional point charges and Hartree-Fock calculations of the “embedded” clusters using a 6–311++G** basis set give a Mulliken charge of $-(0.07\text{--}0.08)$ on the Br^0 atom, which would suppress the preedge feature very little. The same calculation indicates that 92%–95% of the unpaired electron density resides on the bromine atom. Configuration interaction with single excitations calculations for the embedded clusters indicate that weak CT is sufficient to account for the observed absorption band in the ultraviolet⁸ (with a calculated oscillator strength of 0.2 and transition energy of 5.6 eV).

In conclusion, we report the transient x-ray absorption spectrum of the short-lived hydrated Br^0 atom and follow its reaction to form Br_2^- . The solvent shell around Br^0 is defined primarily by weak hydrophobic interactions, with the atom residing within a large “bubble.” Our simulations suggest that a single solvent molecule directly interacts with the atom to form a weak $\sigma^2\sigma^{*1}$ bond. Although charge transfer in the ground state of the Br^0 -water adduct is too weak to noticeably suppress the $1s$ – $4p$ resonance in the x-ray absorption spectrum, the previously observed⁸ CT band for neutral bromine atoms in water supports the formation of an adduct. The XAFS signature of the weak Br^0 -water complex is obscured by scattering from 10–12 unbound water molecules in the hydration shell. This study paves the way to observation and characterization of the solvent structure for other short-lived radical intermediates by means of time-resolved XAS.

We thank S. Ross for help with avalanche photodiode detectors, E. Dufresne and D. Walko for beamline assistance, L. Young and her colleagues for use of their instruments, and P. Jungwirth, C. Bressler, R. Saykally, P. D’Angelo, and S. Bradforth for helpful discussions. Use of the Advanced Photon Source was supported by the U.S. Department of Energy, Office of Basic Energy Sciences, under Contract No. DE-AC02-06CH11357.

¹A. Plech *et al.*, Phys. Rev. Lett. **92**, 125505 (2004).

²C. Bressler *et al.*, J. Chem. Phys. **116**, 2955 (2002).

³C. Bressler and M. Chergui, Chem. Rev. (Washington, D.C.) **104**, 1781 (2004).

⁴L. X. Chen, Angew. Chem., Int. Ed. **43**, 2886 (2004).

⁵W. Gawelda *et al.*, Phys. Rev. Lett. **98**, 057401 (2007).

⁶T. Lee *et al.*, J. Chem. Phys. **122**, 1 (2005).

⁷V.-T. Pham *et al.*, J. Am. Chem. Soc. **129**, 1530 (2007).

⁸A. Treinin and E. Hayon, J. Am. Chem. Soc. **97**, 1716 (1975).

- ⁹M. D. Sevilla *et al.*, J. Phys. Chem. A **101**, 2910 (1997).
- ¹⁰M. Roeselova, U. Kandor, and P. Jungwirth, J. Phys. Chem. A **104**, 6523 (2000).
- ¹¹R. Lian *et al.*, J. Phys. Chem. A **110**, 9071 (2006).
- ¹²See EPAPS Document No. E-JCPSA6-128-024802 for supplementary information. This document can be reached through a direct link in the online article's HTML reference section or via the EPAPS homepage (<http://www.aip.org/pubservs/epaps.html>).
- ¹³D. Zehavi and J. Rabani, J. Phys. Chem. **76**, 312 (1972).
- ¹⁴Y. Wu, H. L. Tepper, and G. A. Voth, J. Chem. Phys. **124**, 024503 (2006).
- ¹⁵P. D'Angelo *et al.*, J. Chem. Phys. **100**, 985 (1994).
- ¹⁶P. J. Merklings *et al.*, J. Chem. Phys. **119**, 6647 (2003).
- ¹⁷A. L. Ankudinov *et al.*, Phys. Rev. B **58**, 7565 (1998).